



Faculty of Girls for Art,
Science and Education,
Ain Shams University

Monte Carlo Study of the Transport Properties in Some Semiconductors

Thesis

**Submitted in the Partial Fulfillment for M.Sc.
Degree in Solid State Physics**

To

**Physics Department
Faculty of Girls for Art, Science and
Education, Ain Shams University**

By

Nesreen Taha Mokhtar

B.Sc. in Physics, *1999*

2005



Faculty of Girls for Art,
Science and Education,
Ain Shams University

Monte Carlo Study of the Transport Properties in Some Semiconductors

Thesis

**Submitted in the Partial Fulfillment for M.Sc.
Degree in Solid State Physics**

To

**Physics Department
Faculty of Girls for Art, Science and
Education, Ain Shams University**

By

Nesreen Taha Mokhtar

B.Sc. in Physics, 1999

Supervisors

Prof. Dr. *Mohyi El - Din Abd El Lattif Kenawy*

Department of Physics,
Faculty of Girls,
Ain Shams University, Cairo, Egypt

Assist. Prof. Dr.

Salwa Moustafa Abd El Wahab

Department of Physics,
Faculty of Girls,
Ain Shams University, Cairo, Egypt

Assist. Prof. Dr.

Fadl Allah Mohammed Abu El - Ela

Department of Physics,
Faculty of Girls,
Ain Shams University, Cairo, Egypt



Faculty of Girls for Art,
Science and Education,
Ain Shams University

Approval sheet

Student Name: ***Nesreen Taha Mokhtar “B.Sc. in Physics, 1999”.***

Thesis Title : ***Monte Carlo Study of the Transport Properties
Sin Some Semiconductors.***

*Submitted in the Partial Fulfillment for M.Sc.
Degree in Solid State Physics.*

Supervisors Committee:

● ***Prof.Dr. Mohyi El-Din Abd El Lattif Kenawy*** - - - - -

Department of Physics,
Faculty of Girls,
Ain Shams University, Cairo, Egypt

● ***Assist.Prof.Dr. Salwa Moustafa Abd El Wahab*** - - - - -

Department of Physics,
Faculty of Girls,
Ain Shams University, Cairo, Egypt

● ***Assist.Prof.Dr. Fadl Allah Mohammed Abu El-Ela*** - - - - -

Department of Physics,
Faculty of Girls,
Ain Shams University, Cairo, Egypt

Date of research: / /

Post Graduate Studies Department

Approval Stamp

Approval Date: / /

Faculty Council Approval

University Council Approval

Date: / /

Date: / /

Dedicated

To

My Parents,

My Sisters,

My Friends,

and

My Sweet Daughter

Mona

Acknowledgement

I humbly kneel to ***ALLAH*** thanking ***HIM*** for showing me the right path, without ***HIS*** help my efforts would have gone astray.

I would like hereby to express my sincere appreciation and gratitude for:

● **Prof. Dr. *Mohyi El-Din Abd El Lattif Kenawy***

Department of Physics,
Faculty of Girls,
Ain Shams University, Cairo, Egypt

● **Assist. Prof. Dr. *Salwa Moustafa Abd El Wahab***

Department of Physics,
Faculty of Girls,
Ain Shams University, Cairo, Egypt

● **Assist. Prof. Dr. *Fadl Allah Mohammed Abu El - Ela***

Department of Physics,
Faculty of Girls,
Ain Shams University, Cairo, Egypt




for their kind supervision, continuous encouragement and fruitful discussions throughout the period of this work.

As well as the whole ***Department of Physics, Faculty of Girls, Ain Shams University*** for their kind support and encouragement during my work.

Contents

Subject	Page
<i>List of Figures</i>	iii
<i>List of Tables</i>	xxi
<i>Abstract</i>	xxiii

Chapter	Contents	Page
1	<i>Introduction</i>	1
2	<i>Transport Theory and Scattering Mechanisms</i>	11
	2.1 Introduction	11
	2.2 The Boltzmann Transport Equation	11
	2.3 Band Structure	17
	2.4 Scattering Mechanisms	23
	2.4.1 Lattice Vibration Scattering	24
	2.4.2 Defect Scattering Mechanism	28
	2.4.3 Carrier – Carrier Scattering	30
3	<i>Theory of Scattering and Total Scattering Rates of Various Scattering Mechanisms</i>	33
	3.1 Theory of Scattering	33
	3.2 Scattering Probabilities	36
	3.2.1 Non-Equivalent Intervalley Phonon Scattering	36
	3.2.2 Equivalent Intervalley Phonon Scattering	42
	3.2.3 Polar Optical Phonon Scattering	46

3.2.4	<i>Intravalley Non-Polar Optical Phonon Scattering</i>	53
3.2.5	<i>Acoustic Phonon Scattering</i>	57
3.2.6	<i>Piezoelectric Phonon Scattering</i>	61
3.2.7	<i>Ionised Impurity Scattering</i>	64
3.2.8	<i>Alloy Scattering</i>	79
4	<i>The Monte Carlo Method and Its Applications in Semiconductors</i>	85
4.1	<i>The Monte Carlo Method</i>	85
4.1.1	<i>Initial Conditions of Motion</i>	89
4.1.2	<i>Free Flight Time</i>	90
4.1.3	<i>Selecting the Scattering Process</i>	93
4.1.4	<i>Selecting the Final State</i>	98
4.1.5	<i>Collecting the Average Transport Quantities ..</i>	101
4.1.6	<i>Ensemble Monte Carlo</i>	101
4.2	<i>Velocity Overshoot</i>	106
5	<i>Results and Discussion</i>	109
5.1	<i>GaAs</i>	112
5.2	<i>InP</i>	136
5.3	<i>GaInAs</i>	157
	<i>Conclusions</i>	181
	<i>References</i>	185
	<i>Summary in Arabic</i>	

List of Figures

Figure	Page
Fig. [2.1]: Schematic representation of the semi-classical trajectory of an electron in $\bar{\mathbf{k}}$ space under the influence of an electric field [<i>Fawcett - 1973</i>]	13
Fig. [2.2]: (a) The <i>First Brillouin Zone</i> for the face-centered cubic, diamond and zinc blende structures. Also shown are symmetry points and directions of the <i>First Brillouin Zone</i> [<i>Shur - 1990</i>].	
(b) Structure of the reduced <i>Brillouin Zone</i> of GaAs [<i>Antoncik - 1973</i>]	18
Fig. [2.3]: The lattice structure of zinc blende crystal [<i>Antoncik - 1973</i>]	19
Fig. [2.4]: Schematic representation of the energy band structure of GaAs in $\langle 000 \rangle$, $\langle 100 \rangle$ and $\langle 111 \rangle$ directions [<i>Blakemore - 1985</i>]	19
Fig. [2.5]: Important minima of the conduction band and maxima of the valence band in cubic semiconductors [<i>Shur - 1990</i>]	20
Fig. [2.6]: (a) Spherical constant energy surface for the lowest G minimum of the conduction band in GaAs in the <i>First Brillouin Zone</i> [<i>Shur - 1990</i>].	
(b) Energy surface contours in the L valley [<i>Antoncik - 1973</i>].	

(c) Energy surface contours in the X valley [<i>Antoncik - 1973</i>]	23
-------------------------------------------------------------------------------------	----

Fig. [2.7]: Dispersion curves for lattice vibrations in semiconductors [<i>Nag - 1980</i>]	27
-----------------------------------------------------------------------------------------------------------	----

Fig. [2.8]: Energy gap in the presence of an acoustic wave [<i>Nag - 1980</i>]	27
-----------------------------------------------------------------------------------------------	----

Fig. [3.1]: The <i>Non-Equivalent Intervalley Phonon Scattering Rate</i> “emission and absorption” as a function of energy at 300 K	
---------------------------------------------------------------------------------------------------------------------------------------------------	--

(a) From the G valley to L and X valleys in GaAs	39
(b) From the G valley to L and X valleys in InP	39
(c) From the G valley to L and X valleys in GaInAs	39
(d) From the L valley to G and X valleys in GaAs	40
(e) From the L valley to G and X valleys in InP	40
(f) From the L valley to G and X valleys in GaInAs	40
(g) From the X valley to G and L valleys in GaAs	41
(h) From the X valley to G and L valleys in InP	41
(i) From the X valley to G and L valleys in GaInAs	41

Fig. [3.2]: The *Equivalent Intervalley Phonon Scattering Rate* as a function of energy at **300 K**

(a) Emission, absorption and total scattering rate in the L valley of GaAs	44
(b) Emission, absorption and total scattering rate in the L valley of InP	44
(c) Emission, absorption and total scattering rate in the L valley of GaInAs	44
(d) Emission, absorption and total scattering rate in the X valley of GaAs	44
(e) Emission, absorption and total scattering rate in the X valley of InP	44
(f) Emission, absorption and total scattering rate in the X valley of in GaInAs	44
(g) Total scattering rate in the L and X valleys of GaAs	45
(h) Total scattering rate in the L and X valleys of InP	45
(i) Total scattering rate in the L and X valleys of GaInAs	45

Fig. [3.3]: The *Polar Optical Phonon Scattering Rate* as a function of energy at **300 K**

(a) Emission, absorption and total scattering rate in the G valley of GaAs	50
(b) Emission, absorption and total scattering rate in the G valley of InP	50
(c) Emission, absorption and total scattering rate in the G valley of GaInAs	50
(d) Emission, absorption and total scattering rate in the L valley of GaAs	50
(e) Emission, absorption and total scattering rate in the L valley of InP	50

(f) Emission, absorption and total scattering rate in the L valley of in GaInAs	50
(g) Total scattering rate in the G , L and X valleys of GaAs	51
(h) Total scattering rate in the G , L and X valleys of InP	51
(i) Total scattering rate in the G , L and X valleys of GaInAs	51

Fig. [3.4]: The angular dependence of the <i>Polar Optical Phonon Scattering</i> probability for electron energies of 0.1 eV and 0.4 eV at 300 K	52
(a) In GaAs .	
(b) In InP .	
(c) In GaInAs .	

Fig. [3.5]: The <i>Non-Polar Optical Phonon Scattering Rate</i> as a function of energy at 300 K	
----------------------------------------------------------------------------------------------------------------	--

(a) Emission, absorption and total scattering rate in the L valley of GaAs	55
(b) Emission, absorption and total scattering rate in the L valley of InP	55
(c) Emission, absorption and total scattering rate in the L valley of GaInAs	55
(d) Emission, absorption and total scattering rate in the X valley of GaAs	55
(e) Emission, absorption and total scattering rate in the X valley of InP	55
(f) Emission, absorption and total scattering rate in the X valley of GaInAs	55
(g) Total scattering rate in the L and X valleys of GaAs	56

(h) Total scattering rate in the L and X valleys of InP	56
(i) Total scattering rate in the L and X valleys of GaInAs	56

Fig. [3.6]: The <i>Acoustic Phonon Scattering Rate</i> as a function of energy in the G , L and X valleys at 300 K	59
(a) In GaAs .	
(b) In InP .	
(c) In GaInAs .	

Fig. [3.7]: The angular dependence of the <i>Acoustic Phonon Scattering</i> probability for electron energies of 0.1 eV and 0.4 eV at 300 K	60
(a) In the G valley of GaAs .	
(b) In the G valley of InP .	
(c) In the G valley of GaInAs .	
(d) In the L valley of GaAs .	
(e) In the L valley of InP .	
(f) In the L valley of GaInAs .	

Fig. [3.8]: The <i>Piezoelectric Phonon Scattering Rate</i> as a function of energy in the G , L and X valleys at 300 K	63
(a) In GaAs .	
(b) In InP .	
(c) In GaInAs .	

Fig. [3.9]: (a) Schematic diagram for <i>Rutherford Scattering</i> [Ridley - 1988]	64
(b) Schematic representation of the electron conservation momentum in <i>Impurity Scattering</i>	

[*Ridley - 1988*] 67

Fig. [3.10]: The *Brooks-Herring* Impurity Scattering Rate as a function of energy in the **G**, **L** and **X** valleys at **300 K** 72

- (a) For electrons with density $1 \times 10^{23} \text{ m}^{-3}$ in **GaAs**.
- (b) For electrons with density $1 \times 10^{23} \text{ m}^{-3}$ in **InP**.
- (c) For electrons with density $1 \times 10^{23} \text{ m}^{-3}$ in **GaInAs**.
- (d) For electrons with density $1 \times 10^{22} \text{ m}^{-3}$ in **GaAs**.
- (e) For electrons with density $1 \times 10^{22} \text{ m}^{-3}$ in **InP**.
- (f) For electrons with density $1 \times 10^{22} \text{ m}^{-3}$ in **GaInAs**.
- (g) For electrons with density $1 \times 10^{21} \text{ m}^{-3}$ in **GaAs**.
- (h) For electrons with density $1 \times 10^{21} \text{ m}^{-3}$ in **InP**.
- (a) For electrons with density $1 \times 10^{21} \text{ m}^{-3}$ in **GaInAs**.

Fig. [3.11]: The *Ridley* Impurity Scattering Rate as a function of energy in the **G**, **L** and **X** valleys at **300 K** 73

- (a) For electrons with density $1 \times 10^{23} \text{ m}^{-3}$ in **GaAs**.
- (b) For electrons with density $1 \times 10^{23} \text{ m}^{-3}$ in **InP**.
- (c) For electrons with density $1 \times 10^{23} \text{ m}^{-3}$ in **GaInAs**.
- (d) For electrons with density $1 \times 10^{22} \text{ m}^{-3}$ in **GaAs**.
- (e) For electrons with density $1 \times 10^{22} \text{ m}^{-3}$ in **InP**.
- (f) For electrons with density $1 \times 10^{22} \text{ m}^{-3}$ in **GaInAs**.
- (g) For electrons with density $1 \times 10^{21} \text{ m}^{-3}$ in **GaAs**.
- (h) For electrons with density $1 \times 10^{21} \text{ m}^{-3}$ in **InP**.
- (i) For electrons with density $1 \times 10^{21} \text{ m}^{-3}$ in **GaInAs**.

- Fig. [3.12]:** A comparison between the *Brooks-Herring Model* for carrier concentration $1 \times 10^{21} \text{ m}^{-3}$ and the *Ridley Model* for carrier concentrations $1 \times 10^{21} \text{ m}^{-3}$, $1 \times 10^{22} \text{ m}^{-3}$ and $1 \times 10^{23} \text{ m}^{-3}$ in the **G** valley at **300 K** 74
- (a) In **GaAs**.
 (b) In **InP**.
 (c) In **GaInAs**.
- Fig. [3.13]:** A *Brooks-Herring Model* at **77 K** and **300 K** in the **G** valley for carrier concentration $1 \times 10^{23} \text{ m}^{-3}$ 76
- (a) In **GaAs**.
 (b) In **InP**.
 (c) In **GaInAs**.
- Fig. [3.14]:** A *Ridley Model* at **77 K** and **300 K** in the **G** valley for carrier concentration $1 \times 10^{23} \text{ m}^{-3}$ 77
- (a) In **GaAs**.
 (b) In **InP**.
 (c) In **GaInAs**.
- Fig. [3.15]:** The *Alloy Scattering Rate* as a function of energy in the **G**, **L** and **X** valleys of **Ga_{0.47}In_{0.53}As** at **300 K** 80
- Fig. [3.16]:** Scattering rates for all scattering mechanisms as a function of energy in the **L** valley of **GaAs** at **300 K** 81
- Fig. [3.17]:** Scattering rates for all scattering mechanisms as a function of energy in the **L** valley of **InP** at **300 K** 82

Fig. [3.18]: Scattering rates for all scattering mechanisms as a function of energy in the L valley of GaInAs at 300 K	83
Fig. [4.1]: Flow chart for a <i>Monte Carlo</i> simulation [<i>Littlejohn et. al. - 1982</i>]	88
Fig. [4.2]: Diagram showing the selection of the scattering process [<i>Hockney & Eastwood - 1981</i>]	94
Fig. [4.3]: The total scattering rate for the electrons in <i>Band I</i> and <i>Band II</i> as a function of wave number [<i>Hockney & Eastwood - 1981</i>]	95
Fig. [4.4]: Representation for the electron coordinates	102
Fig. [4.5]: Sketch illustrating the synchronous-ensemble method [<i>Jacoboni & Reggiani - 1983</i>]	103
Fig. [4.6]: A typical electron orbit for a high scattering rate, showing several free flights per field-adjusting time step [<i>Hockney & Eastwood - 1981</i>]	104
Fig. [5.1]: The total and average electron drift velocity versus electric field in the G and L valleys of GaAs	114
(a) At lattice temperature of 77 K .	
(b) At lattice temperature of 150 K .	
(c) At lattice temperature of 300 K .	